# Atomic recombination in a hypersonic wind-tunnel nozzle

By K. N. C. BRAY
Department of Aeronautical Engineering, University of Southampton

(Received 30 October 1958)

The flow of an ideal dissociating gas through a nearly conical nozzle is considered. The equations of one-dimensional motion are solved numerically assuming a simple rate equation together with a number of different values for the rate constant. These calculations suggest that deviations from chemical equilibrium will occur in the nozzle if the rate constant lies within a very wide range of values, and that, once such a deviation has begun, the gas will very rapidly 'freeze'. The dissociation fraction will then remain almost constant if the flow is expanded further, or even if it passes through a constant area section. An approximate method of solution, making use of this property of sudden 'freezing' of the flow, has been developed and applied to the problem of estimating the deviations from equilibrium under a wide range of conditions. If all the assumptions made in this paper are accepted, then lack of chemical equilibrium may be expected in the working sections of hypersonic wind tunnels and shock tubes. The shape of an optimum nozzle is derived in order to minimize this departure from equilibrium.

It is shown that, while the test section conditions are greatly affected by 'freezing', the flow behind a normal shock wave is only changed slightly. The heat transfer rate and drag of a blunt body are estimated to be reduced by only about 25 % even if complete freezing occurs. However, the shock wave shape is shown to be rather more sensitive to departures from equilibrium.

## 1. Introduction

In attempting to simulate the conditions of high velocity flight it has become necessary to devise wind tunnels with very high stagnation enthalpies. Such facilities may vary widely in their mode of operation. Typical examples, in order of increasing stagnation temperature, are: tunnels with storage heaters, Smelt (1955); tunnels with piston-type compression heaters, Cox & Winter (1957); electric arc discharge tunnels, Lukasiewicz (1958); and shock-tube wind tunnels, Hertzberg (1957). All these tunnels have in common the fact that they produce a high velocity flow by expanding the gas through a nozzle; this converts the thermal energy of random molecular motion into directed kinetic energy of the high speed flow. The amount of energy required is very large, so the temperature of the unexpanded gas must be high, and this means that the vibrational energy modes of the molecules will be excited to high levels so that the gas will be partially dissociated and perhaps ionized.

The flow through the nozzle is hypersonic, and so the rate of fall of temperature following the gas through the nozzle may be very large. As the temperature falls a wide variety of internal adjustments must continually be made by means of molecular collisions. The energy level of molecular vibrations must be reduced, a new balance must be found between atoms and molecules, chemical reactions must take place between the different species present and ions must recombine to form neutral particles. All these adjustments require a large number of collisions between molecules before they can reach equilibrium. If the time to reach equilibrium is of the same order of magnitude as the time for a typical molecule to pass through the nozzle, then departures from equilibrium are to be expected, which may modify the flow pattern.

These so-called relaxation effects can occur whenever the temperature changes so fast that the internal structure of the gas cannot keep pace; other examples of interest to aerodynamicists are the flow round the 'shoulder' of a blunt body in hypersonic flight and the flow through a strong shock wave. The latter problem has received considerable attention both theoretically (Wood 1956; Evans 1956; Freeman 1958; Duff 1958) and experimentally (Hertzberg 1957; Rose 1957; Byron 1957). Many attempts have been made to deduce the rate constants for the various relaxation processes from shock wave experiments, and some degree of success has been achieved. However, there is still considerable uncertainty about some of the rates of reaction (particularly those for dissociation), and also about their variation with temperature.

Two conditions must be satisfied if the relaxation of a particular degree of freedom is to affect the flow through a nozzle: the relaxation time must be comparable in magnitude with the time for the flow to pass through the nozzle, and the change in energy associated with the relaxing mode must form a significant part of the total change of enthalpy of the gas. Heims (1958) has applied these conditions to the flow of oxygen through a nozzle. He concludes that vibrational relaxation effects will be small compared with dissociation effects because of the energy condition, even though the relaxation times may be comparable at high temperatures. Byron (1957) has reached the same conclusion as a result of shock-tube experiments.

Similar arguments suggest that effects of ionization relaxation will also be small until the temperature becomes large enough for a significant amount of energy to be involved in ionization. It therefore appears that the dissociation and recombination of oxygen and nitrogen molecules and the formation and dissociation of oxides of nitrogen will be the most important relaxation effects to be considered. The possibility of interactions between different molecular energy modes must, however, be remembered.

The present work is concerned with only one type of relaxation phenomenon. Its object is to estimate the effects of finite rates of molecular dissociation and recombination on the performance of hypersonic wind-tunnel nozzles, and to establish a suitable criterion for the conditions under which these rates will be important. The ideal dissociating gas of Lighthill (1957) and Freeman (1958), which is discussed in detail in the next section, is used throughout. This simplified model of the gas behaviour cannot be expected to give accurate quantitative

results in the present application, but it does represent the main features of a dissociating gas with sufficient simplicity to allow the problem to be formulated.

It is hoped that the criterion for equilibrium which is deduced here may later be applied to more accurate calculations, involving real gas properties.

The equations for the quasi-one-dimensional frictionless adiabatic flow of an ideal dissociating gas have been set up and solved for a number of different values of the reaction rate parameter. From these calculations it is deduced that the flow through a nozzle will 'freeze' under certain conditions, when the rate of recombination of atoms to form molecules is too small to maintain equilibrium. Calculations have been made only for the wind-tunnel case in which the flow is accelerated from rest through a convergent-divergent nozzle. However, the problem of the hypersonic shock tube, in which an already supersonic flow is expanded through a divergent nozzle, is also discussed, and it is shown that relaxation effects will be exactly the same as in the wind-tunnel case if the reaction rate parameter is greater than a certain value.

At temperatures for which dissociation is important, the rate of loss of heat from a gas by radiation is believed to be large. However, the energy radiated per unit mass of gas is a very strong function of the gas temperature, so that most of this radiation will take place in the stagnation region ahead of the nozzle throat, where the temperature is highest. Radiation is therefore neglected in the following calculations, it being assumed that the stagnation enthalpy has been reduced by an appropriate amount to allow for losses in the stagnation region.

No allowance is made for viscous effects, although these also are known to be very large in hypersonic nozzles. However, it seems reasonable to hope that there will be an inviscid core of flow in a real nozzle, for which an effective area ratio may be defined, and to which the one-dimensional adiabatic flow equations will apply. Also, the rate equations near the walls will be greatly modified by the possibility of collisions between atoms or molecules and the walls; for this reason recombination is likely to be much more rapid near the walls, but these recombined molecules can only diffuse out from the walls at a finite rate, so they can only affect the flow within the boundary layer. The central core of adiabatic flow will be unaffected.

Because hypersonic nozzles employ small expansion angles, and also because boundary layer effects are known to be so large, reducing the effective expansion angle still further, a quasi-one-dimensional flow theory should be sufficiently accurate for the present purpose. The extra complication involved in allowing for velocity components normal to the nozzle axis does not appear to be justified at this stage.

Relaxation phenomena in nozzles have been studied by Penner (1955), Logan (1957), Heims (1958) and many others. Penner, together with co-workers, has derived linearized theories for flows close to dissociation equilibrium and flows which are nearly frozen in their initial composition. From these he has derived simple criteria to determine the equilibrium state of the exhaust gases from a rocket nozzle. Logan (1957) applies a similar method to atomic recombination in a hypersonic wind tunnel. He assumes that departure from equilibrium will occur in regions where the rate of change of temperature is large, and uses the results

of Penner (1955) which were derived for flow in rocket nozzles. He takes as the criterion for the flow to be near equilibrium:

$$\frac{1}{T}\frac{dT}{dt}\tau_{\max} \leqslant 10^{-3}.$$

Here $T$ is the actual value of the local temperature, $dT/dt$ is the rate of change of temperature with respect to time, and $\tau_{\max}$ is the maximum value of the reaction time for the chemical process, that is the time to reach a value $(1-1/e)$ times the equilibrium concentration. On the basis of this criterion, Logan predicts large departures from equilibrium in a hypersonic wind-tunnel nozzle where the rate of cooling can be very high. The lack of equilibrium is predicted to occur in the early part of the nozzle where $dT/dt$ is large. This so-called 'frozen' flow region is followed by an adjustment zone where equilibrium is regained by a sudden irreversible release of the dissociation energy with a large increase of entropy and an even larger decrease in the Mach number.

The present calculations suggest that, once an appreciable deviation from dissociation equilibrium has occurred in a hypersonic nozzle, a return to equilibrium is unlikely to take place within the nozzle. This must be compared with Logan's assumption that the region of partially frozen flow is followed by another zone in which full equilibrium is achieved.

These conflicting results may be understood when it is realized that the conditions in a rocket nozzle, with an area ratio of three or four, are very different from those in a hypersonic nozzle, which may have an area ratio of several thousand. The fall of density is therefore several orders of magnitude greater in the wind-tunnel nozzle than in the rocket case, and this has a large effect on the rate of atomic recombination, which requires a three-body collision process and so depends on the density squared. It follows that an equilibrium criterion giving good results in the rocket nozzle case, where the density change is not large, will not be suitable for application to the nozzle of a hypersonic wind tunnel.

## 2. The ideal dissociating gas

The thermodynamic changes in a real gas at high temperatures are extremely complicated and not very well understood in detail. In order that gas dynamic theories may be at all general in application, it is necessary to find simple equations which will describe the changes of state of all gases with reasonable accuracy within a specified range of temperatures and pressures. The ideal dissociating gas of Lighthill (1957) does just this, within the range of conditions where dissociation is the dominant effect.

If a partially dissociated gas, in conditions of thermal equilibrium, be regarded as a mixture of two perfect gases, the molecules and the atoms, then the equation of state for the mixture may be written

$$p' = \frac{k}{2m}\rho' T'(1+\alpha), \tag{1}$$

where $p'$ is the pressure, $\rho'$ the density, $T'$ the temperature, $\alpha$ the ratio by mass of atoms dissociated to total of atoms and molecules; $k$ is Boltzmann's constant and $m$ is the mass of an atom.

The law of mass action, which determines the equilibrium composition of the mixture of atoms and molecules, is (for a perfect gas)

$$\frac{\alpha^2}{1-\alpha} = \frac{\rho'_d}{\rho'} e^{-D/kT'}, \tag{2}$$

where $\rho'_d$ is a characteristic density which is a complicated function of the temperature. Lighthill shows that it is a reasonable approximation to take $\rho'_d$ = constant over a wide range of temperatures for both oxygen and nitrogen. This greatly simplifies the problem; it is consistent with taking the vibrational degrees of freedom of the molecules as always being half-excited, even at low temperatures, and leads to the expression

$$u' = \frac{3k}{2m} T' + \frac{D}{2m} \alpha \tag{3}$$

for the internal energy per unit mass, where $D$ is the energy of dissociation. The specific enthalpy is then given by

$$i' = u' + \frac{p'}{\rho'} = (4+\alpha) T' \frac{k}{2m} + \frac{D}{2m} \alpha. \tag{4}$$

It will be seen that, as $\alpha$ approaches zero at low temperature, the ideal dissociating gas becomes a perfect gas with constant specific heats and with $\gamma = c_p/c_v = \frac{4}{3}$. This incorrect low-temperature behaviour sets a lower limit below which air cannot be accurately represented by an ideal dissociating gas. An upper limit will also be fixed by the fact that electronic contributions to internal energy are neglected, as is ionization.

Lighthill sets these lower and upper limits at approximately 3000 and 7000 °K for oxygen and nitrogen with densities between $10^{-3}$ and 1 of N.T.P. However, the ideal dissociating gas may be expected to show trends correctly over a much wider range of conditions, and if necessary corrections can be made at high and low temperatures. At low temperatures, the rate of change of temperature with area ratio in a one-dimensional flow will be too small, because $\gamma$ is too small. Neglecting electronic excitation and ionization will make the calculated temperature too high for very hot gases, because the electronic contributions to internal energy and ionization energy have not been allowed for in full.

Following Lighthill, we define a characteristic temperature, density, pressure, internal energy and velocity for the gas (values of these quantities for oxygen and nitrogen are given in table 1):

$$\left.\begin{aligned} T'_d &= D/k, \\ \rho'_d &= \text{constant}, \\ p'_d &= \rho'_d D/2m, \\ u'_d &= D/2m, \\ v'_d &= \sqrt{(D/2m)}. \end{aligned}\right\} \tag{5}$$

We now write equations (1), (2), (3) and (4) in terms of the dimensionless quantities $T$, $\rho$, $p$ and $u$, using $T'_d$, $\rho'_d$, $p'_d$ and $u'_d$ as units:

$$p = \rho T(1+\alpha), \tag{6}$$

$$\frac{\alpha^2}{1-\alpha} = \frac{1}{\rho} e^{-1/T}, \tag{7}$$

$$u = 3T + \alpha, \tag{8}$$

$$i = (4+\alpha)T + \alpha. \tag{9}$$

These equations completely specify the thermodynamic behaviour of the ideal dissociating gas in equilibrium.

| Quantity | Units | Oxygen | Nitrogen |
|---|---|---|---|
| $T'_d$ | °K | 59,000 | 113,000 |
| $\rho'_d$ | g/cm$^3$ | 150 | 130 |
| $p'_d$ | atm. | $2{\cdot}3 \times 10^7$ | $4{\cdot}1 \times 10^7$ |
| $i'_d$ | kcal./g | 3·67 | 8·02 |
| $v'_d$ | km/sec | 3·9 | 5·8 |

TABLE 1. Characteristic dissociation quantities for oxygen and nitrogen (Lighthill 1957)

Lighthill's equilibrium theory has been extended by Freeman (1958) to cases where equilibrium is not achieved. Freeman writes the net rate of dissociation as

$$\frac{d\alpha}{dt} = r_D - r_R, \tag{10}$$

where $r_D$ is the rate of dissociation and $r_R$ is the rate of recombination.

Dissociation takes place when the energy in the internal degrees of freedom of a molecule is increased by means of collisions with other particles to a level which is sufficient to overcome the binding forces which hold the atoms together. The energies of molecular rotation and vibration may contribute towards making dissociation possible, as well as the relative translational energies of the molecules. Freeman therefore assumes that $r_D$ is proportional to the number of binary collisions involving sufficient total energy to cause dissociation, so that

$$r_D = C_1(\alpha, T')\rho'(1-\alpha)\, e^{-D/kT'},$$

where $C_1(\alpha, T')$ is an unknown function which is related to the dissociation rate constant $k_D$ of chemical kinetics. Freeman concludes that the variation of $C_1$ with $\alpha$ is unimportant compared with its variation with $T'$. He takes this variation to be a negative power of $T'$, such that

$$C_1 = C'(T')^{-s},$$

where $C'$ is a rate constant. This temperature variation is appropriate to a system in which $n$ classical degrees of freedom of the two particles combine to make dissociation possible, where

$$s = \tfrac{1}{2}n - 1.$$

Freeman counts the relative translational energy of both particles but the rotational and vibrational energies of only one colliding molecule, on the grounds that the vibrational energies are not fully excited and that molecules sometimes

collide with free atoms, and that a collision may not always use all the available energy. This gives $n = 7$ and $s = 2{\cdot}5$, which appears to be the maximum likely value of this parameter. Byron (1957) shows that $n = 6$ ($s = 2$) gives a better agreement with his shock-tube measurements. Values of $s$ between $-0{\cdot}5$ and $2{\cdot}5$ are considered in this paper, but it is shown that the precise value is not critically important in the present application.

Then
$$r_D = C'\rho'(1-\alpha)\,(T')^{-s}\,e^{-D/kT'},$$
and it follows from the equilibrium condition (equation (2)) that
$$r_R = C'\frac{1}{\rho'_d}(\rho')^2\,(T')^{-s}\,\alpha^2.$$
The rate of recombination is proportional to $(\rho')^2$ because recombination is a process which requires a three-body collision.

Equation (10) now becomes
$$\frac{d\alpha}{dt} = C'\rho'(T')^{-s}\left\{(1-\alpha)\,e^{-D/kT'} - \frac{\rho'}{\rho'_d}\alpha^2\right\}. \tag{11}$$

This rate equation may not be accurate. Its derivation is based on simple collision theory which probably does not give a correct detailed picture of the reaction process. For example, Frood (see Winter (1958)) has argued that the net dissociation rate must depend on all the particles present, and on all their energy states. Thus the existence of a small number of free electrons, or a few molecules with very high rotational energy levels, can have a large effect on the overall reaction rate. Also, it is believed that the passage of a strong shock wave through air may cause initial over-dissociation of the oxygen, followed by recombination as the temperature falls further downstream owing to the continued dissociation of nitrogen molecules. Unfortunately, a rate equation embodying all these effects is not at present available, so we can only hope that equation (11) may not lead us too far astray if the parameters $C'$ and $s$ are suitably chosen for a limited range of conditions.

However, it is encouraging to note that the results of the numerical calculations which are described in this paper appear to be dominated by the term $e^{-D/kT'}$ in $r_D$ for the upstream part of the nozzle; further downstream where $r_D$ has become small the results are dominated by the $(\rho')^2$ in $r_R$. Both of these terms may be expected to occur in a more complicated rate equation, and this suggests that equation (11) may be adequate for our purpose.

## 3. Quasi-one-dimensional flow equations

The frictionless adiabatic flow of an ideal dissociating gas through a duct of slowly varying cross-sectional area $A'$ is described by the equations of conservation of mass, momentum and energy:
$$\rho v A' = \rho^* v^* A^*, \tag{12}$$
$$v\frac{dv}{dx'} + \frac{1}{\rho}\frac{dp}{dx'} = 0, \tag{13}$$
$$i + \tfrac{1}{2}v^2 = i_0, \tag{14}$$

together with the thermodynamic relationships of equations (6) and (9) and the rate equation (11), which may be written in the form

$$\frac{d\alpha}{dt} = C\rho\left(\frac{T}{T_0}\right)^{-s}\{(1-\alpha)\,e^{-1/T} - \alpha^2\rho\}. \tag{15}$$

Quantities at a sonic throat are denoted by ( )*, and $i_0$ is the stagnation enthalpy, which is constant for adiabatic flow. The equations are written in terms of the dimensionless quantities which were introduced in equations (5). A term $T_0^s$ has been introduced into equation (15) for convenience, and $C$ is a reaction rate constant with the dimensions of (time)$^{-1}$. It is related to the recombination rate constant $k_R$ of chemical kinetics by the approximate equation

$$C = k_R\frac{\rho_d'^2}{m^2}\left(\frac{T'}{T_0'}\right)^s.$$

The momentum and continuity equations may be written in terms of a reduced sound speed $a$ defined in the usual way as $\left(\frac{dp/dx'}{d\rho/dx'}\right)^{\frac{1}{2}}$ so that

$$a^2 = \frac{T}{3}(4+\alpha)(1+\alpha) - \frac{d\alpha/dx'}{d\rho/dx'}\frac{\rho}{3}(1+\alpha-3T), \tag{16}$$

and from equations (12) and (13)

$$\frac{1}{A'}\frac{dA'}{dx'} = \frac{1}{\rho v^2}\frac{dp}{dx'}\left(1-\frac{v^2}{a^2}\right). \tag{17}$$

This shows that $a$ is the velocity at which the stream tube area is a minimum, that is, the velocity at a sonic throat as in normal one-dimensional flow theory. Note that $a$ depends not only on the variables of state but also on their derivatives. However, equation (17) may be rewritten

$$\frac{1}{A'}\frac{dA'}{dx'} = \frac{1}{\rho v^2}\frac{dp}{dx'}\left(1-\frac{v^2}{c^2}\right) - \frac{d\alpha}{dx'}\left[\frac{1+\alpha}{3c^2} - \frac{3}{(1+\alpha)(4+\alpha)}\right] \tag{18}$$

in terms of a reduced velocity $c$ defined by

$$c^2 = \frac{T}{3}(4+\alpha)(1+\alpha); \tag{19}$$

clearly, $c$ depends only on variables of state and not on their derivatives. Equation (18) shows that $c$ is the velocity at which $dp/dx'$ cannot be obtained from the continuity and momentum equations. This is important for the one-dimensional flow calculations which follow, because it means that the critical point, which in conventional flow through a convergent-divergent nozzle occurs at the sonic throat where $v = a$, will now occur at another point away from the throat, where $v = c$.

The velocity $c$ is also important in the theory of characteristics for relaxing gases (Boa-Teh Chu 1957; Resler 1957). The equations of two-dimensional steady flow in streamline co-ordinates may be reduced to four simultaneous partial differential equations in the velocity $v$, its direction $\psi$, the pressure $p$ and the dissociation fraction $\alpha$. Four characteristic directions may be found for this

system of equations. Two of these turn out to be coincident with the streamline direction, while the other two are at angles to the streamline direction given by

$$\pm\left[\frac{c^2}{v^2-c^2}\right]^{\frac{1}{2}},$$

so that $c$ rather than $a$ is the velocity component normal to characteristic directions. The equations of motion along these two directions become the pair of ordinary differential equations

$$\frac{\partial\psi}{\partial\sigma} = \mp\left(\frac{v^2}{c^2}-1\right)^{\frac{1}{2}}\frac{1}{\rho v^2}\frac{\partial p}{\partial\sigma} \mp \frac{\rho f c}{p v^2}\left\{\frac{1+\alpha}{4+\alpha} - \frac{p}{\rho}\frac{3}{(4+\alpha)(1+\alpha)}\right\}, \tag{20}$$

where $\partial/\partial\sigma$ means differentiation along one of the characteristic directions defined above, and $f$ is the rate function given in equation (15). The momentum and rate of dissociation equations apply as ordinary differential equations along the other two characteristic directions (the streamlines). This system of equations could be solved by the usual numerical methods.

Boa-Teh Chu (1957) has explained in detail the difference between the velocities $a$ and $c$. He has shown that, for a disturbance propagating in a gas mixture close to equilibrium, $c$ is the velocity of propagation of the wave front while $a$ is the velocity of the bulk of the disturbance. This result is relevant to §7 of the present paper, which discusses the effects of lack of equilibrium in a wind-tunnel nozzle on various quantities which can be measured in the test section of the tunnel. One of the quantities considered is the angle to the flow direction formed by a weak wave, which is shown to be very sensitive to the amount of freezing in the nozzle, and the question arises as to whether such a wave propagates with velocity $a$ or $c$. It is shown, however, that the numerical difference between these quantities is likely to be small under typical conditions.

Equations (12) to (15) cannot be solved until the nozzle shape is specified, so that $d\alpha/dt$ in equation (15) may be written in terms of $d\alpha/dA'$. Many hypersonic wind-tunnel nozzles at the present time are axi-symmetric, with a conical contraction and expansion joined by a cylindrical throat. This throat shape is not suitable for theoretical study as the sharp corners between the conical and cylindrical parts lead to discontinuities in the theoretical flow which will in practice be smoothed out by boundary layer effects. In order to obtain a valid solution through the throat, a nozzle with the hyperbolic area distribution:

$$A' = A^* + K_N^2(x')^2$$

was chosen for these calculations, where $x'$ is the axial distance from the throat and $K_N$ is a constant. It will be seen that, at large distances from the throat, the nozzle becomes indistinguishable from a cone with half angle $\theta$ where

$$\theta = \tan^{-1}\frac{K_N}{\sqrt{\pi}}.$$

We proceed to define an area ratio

$$A = \frac{A'}{A^*}$$

and a dimensionless axial distance

$$\xi = \frac{K_N x'}{\sqrt{A^*}}$$

so that the nozzle shape becomes

$$A = 1 + \xi^2. \tag{21}$$

The system of seven equations, (6), (9), (12), (13), (14), (15), (21), may then be reduced to two simultaneous differential equations in $\alpha$ and $i$, with $\xi$ as independent variable. These are

$$\frac{d\alpha}{d\xi}\left[1 - \frac{3(i-\alpha)}{(1+\alpha)(4+\alpha)}\right] + \frac{di}{d\xi}\left[\frac{\frac{6i_0}{1+\alpha} - \left(\frac{7+\alpha}{1+\alpha}\right)i + \alpha}{2(i_0 - i)}\right] + \frac{2\xi(i-\alpha)}{1+\xi^2} = 0, \tag{22}$$

$$\frac{d\alpha}{d\xi} = \frac{\Phi\rho^* v^* T_0^s \left(\frac{4+\alpha}{i-\alpha}\right)^s}{(1+\xi^2)(i_0 - i)} \left\{(1-\alpha)\, e^{-(4+\alpha)/(i-\alpha)} - \frac{\alpha^2 \rho^* v^*}{(1+\xi^2)\sqrt{[2(i_0 - i)]}}\right\}, \tag{23}$$

where

$$\Phi = \frac{C}{2K_N}\sqrt{\left(\frac{A^*}{D/2m}\right)}$$

is a dimensionless dissociation rate parameter which contains the linear dimensions of the nozzle and its expansion angle as well as the chemical properties of the gas. It may be written approximately in the alternative form

$$\Phi = x_t' \frac{C}{2}\sqrt{\frac{2m}{DA_t}}, \tag{24}$$

where $x_t'$ is the dimensional length of the nozzle and $A_t$ is its exit area ratio.

As pointed out above, some uncertainty still exists about the values of the dissociation rate constants $C$ and $s$. Wood (1956) using a simple collision theory takes $s = -\frac{1}{2}$, whereas Heims (1958) after some discussion of the various theories chooses $s = \frac{1}{2}$. Experimental evidence is not conclusive, but the shock-tube experiments of Byron (1957) in argon-oxygen mixtures are correlated by $s = 2$. It is shown in this paper that the value of $s$ is not important in the type of flow considered here, so $s = 0$ has been used for most of the calculations. The rate constants $C$ of Wood (1956) using simple collision theory, and Heims (1958) using the theory of Wigner (1939), have been adjusted to $s = 0$ taking a mean temperature of 3000 °K for oxygen and 5000 °K for nitrogen. With these adjustments Wood's values are $3{\cdot}8 \times 10^{14}$ per second for oxygen and $1{\cdot}8 \times 10^{15}$ per second for nitrogen; Heims's value for oxygen is $7{\cdot}5 \times 10^{17}$ per second. Shock-tube experiments by Byron (1957) give $C$ the value of $3{\cdot}0 \times 10^{16}$ per second for oxygen, which is intermediate between the theoretical estimates of Wood and Heims. Byron also found that the rate constant for oxygen dissociation was not greatly affected by the presence of nitrogen. Another set of measurements in a shock tube reported by Rose (1957) indicate dissociation rate constants for both oxygen and nitrogen that are of the same order as Heims's oxygen value, but essentially independent of temperature ($s = 0$). In view of all this uncertainty, it is necessary to consider several values of both the rate constants in the calculations which follow.

Figure 1 shows the values of $\Phi$ for oxygen which are obtained from equation (24) for various nozzle lengths and area ratios using the rate constants of Wood (1956) and Heims (1958) with $s = 0$. Also marked on this figure are the nozzles of the Southampton University hypersonic wind tunnel (Bray, Pennelegion & East 1958) and the 16 in. 'Hotshot' tunnel at A.E.D.C., Tullahoma (Lukasiewicz 1958), which may be taken as typical of very small and large installations, respectively.

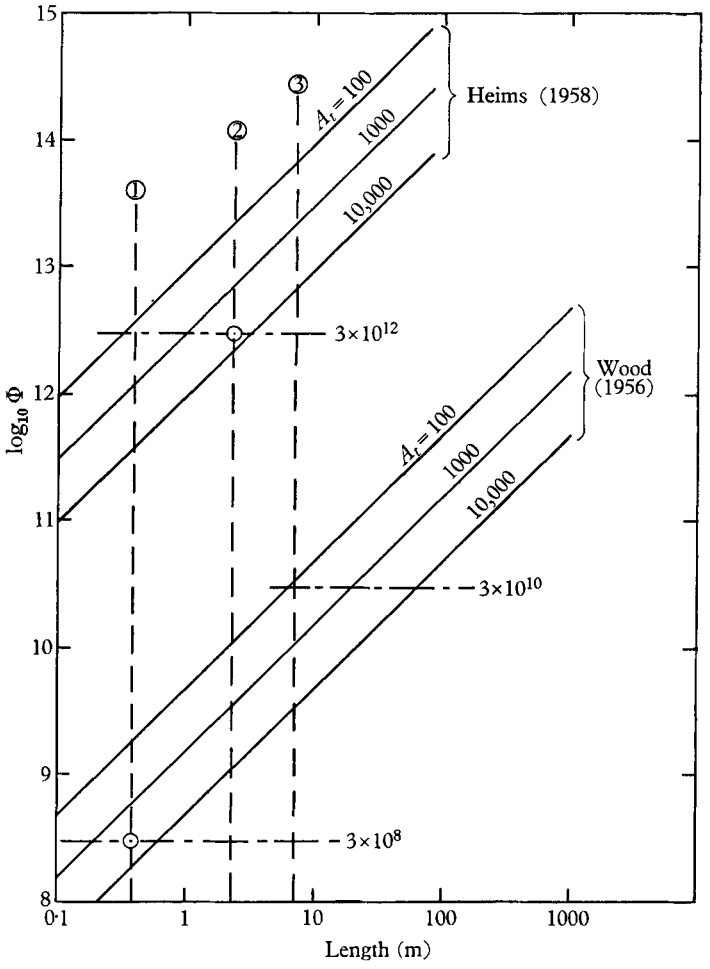


FIGURE 1. The dissociation rate parameter for oxygen in conical nozzles. 1, Southampton hypersonic tunnel; 2, 16 in. hotshot; 3, 50 in. hotshot.

It will be seen that the range of interest for $\Phi$ lies roughly between $3 \times 10^8$ (Southampton tunnel, Wood's rate constant) and $3 \times 10^{12}$ (16 in. 'Hotshot' tunnel, Heims's rate constant) for oxygen dissociation, and perhaps somewhat larger for nitrogen. We will therefore consider values of $\Phi$ within the limits

$$3 \times 10^8 \leqslant \Phi \leqslant 3 \times 10^{13},$$

but it must be remembered that the experimental data on dissociation rates is not yet as reliable as one could wish, and that these limits may have to be modified.

The differential equations (22) and (23), which describe the relaxing one-dimensional flow of an ideal dissociating gas, cannot in general be solved analytically. However, in the limiting case of a gas for which $\Phi = 0$, that is, one for which the net rate of dissociation is negligibly small (frozen flow), equation (23) shows that the dissociation fraction $\alpha$ remains constant at its value at the entrance to the nozzle ($\alpha_0$). Equation (22) can then be integrated to give

$$\pm \ln(1+\xi^2) = -G \ln \frac{i-\alpha_0}{i_0-i} - \frac{1}{4}\left(\frac{7+\alpha_0}{1+\alpha_0}\right) \ln\{(i-\alpha_0)(i_0-i)\} + \text{constant}, \quad (25)$$

where
$$G = \frac{1}{2(i_0-\alpha_0)}\left[\frac{6i_0}{1+\alpha_0} + \alpha_0 - \tfrac{1}{2}(i_0+\alpha_0)\frac{7+\alpha_0}{1+\alpha_0}\right].$$

The constant is determined from conditions at a sonic throat, where $\xi = 0$ by definition and

$$i^* = \frac{1+\alpha_0}{7+\alpha_0}\left[\alpha_0 + \frac{6i_0}{1+\alpha_0}\right]$$

from equation (22), so that $(di/d\xi)^*$ shall not be zero. It may also be derived from equations (14) and (16).

The other limiting case, in which the reaction rate is so fast that equilibrium is reached everywhere in the flow, is given by letting $\Phi$ approach infinity in equation (23). Then, either

$$\frac{d\alpha}{d\xi} \to \infty \quad \text{or} \quad (1-\alpha)\, e^{-(4+\alpha)/(i-\alpha)} = \frac{\alpha^2 \rho^* v^*}{(1+\xi^2)\sqrt{[2(i_0-i)]}}.$$

The latter is the law of mass action (equation (7)) for equilibrium. Together with the condition that the flow is isentropic, it yields the equation

$$3\ln T + \frac{1+\alpha}{T} + \alpha + 2\ln\frac{\alpha}{1-\alpha} = \text{constant}. \quad (26)$$

Hence, from the flow equations (12), (13) and (14), an expression for $d\alpha/d\xi$ may be deduced

$$\frac{d\alpha}{d\xi} = \left(\frac{\xi}{1+\xi^2}\right) \frac{A(\alpha, T)}{B(\alpha)T^3 + C(\alpha)T^2 + D(\alpha)T - E(\alpha)}, \quad (27)$$

where
$$A(\alpha, T) = 4\alpha T(1+\alpha-3T)(1-\alpha)(i_0-i),$$
$$B(\alpha) = (7+\alpha)(4+\alpha)(2-\alpha) - 3\alpha(1-\alpha),$$
$$C(\alpha) = 2\alpha(1-\alpha)(1+\alpha) - 6(2-\alpha)(i_0-\alpha),$$
$$D(\alpha) = 3\alpha(1-\alpha)(3+\alpha),$$
$$E(\alpha) = 2\alpha(1-\alpha)(i_0-\alpha),$$

and
$$i = (4+\alpha)T + \alpha.$$

Equation (27) shows that $d\alpha/d\xi \to 0$ as $\xi \to 0$ unless

$$B(\alpha^*)T^{*3} + C(\alpha^*)T^{*2} + D(\alpha^*)T^* - E(\alpha^*) = 0, \quad (28)$$

and this therefore yields a relation between $\alpha^*$ and $T^*$ at a sonic throat. A simultaneous solution of this and equation (26) gives $\alpha^*$ and $T^*$. The mass flow rate $\rho^* v^*$ follows from equations (7), (9) and (14). Finally, for every equilibrium

condition satisfying equation (26) a value of $\xi$ can be found from the continuity equation (12)

$$\rho v(1+\xi^2) = \rho^* v^*$$

and the equilibrium flow can be solved.

Conditions a long way upstream of the throat ($\xi \to -\infty$) can be studied by expanding $\alpha$, $T$, $\rho$, $p$, $i$ and $v$ as power series in $A^{-\frac{1}{2}}$ and substituting in equations (6), (9), (12), (13), (14), (15) and (21). From this it can be shown that the flow in this region is independent of $\Phi$ to the order $A^{-2}$, so long as $\Phi$ is not identically zero. In other words, the solution to equations (22) and (23) for this region is the equilibrium solution, independent of $\Phi$. This is also to be expected physically, of course, since the velocity is small far upstream of the throat.

## 4. Exact solutions

Solutions of the differential equations (22) and (23) have been found numerically by a step-by-step procedure for one set of stagnation conditions and a number of different values of the rate parameters $\Phi$ and $s$. The stagnation conditions considered were $T_0 = 0{\cdot}1$ and $p_0 = 5 \times 10^{-6}$; equivalent dimensional values of these and the other stagnation quantities for oxygen and nitrogen are given in table 2.

| Quantity | Units | Oxygen | Nitrogen |
|---|---|---|---|
| $T_0'$ | °K | 5,900 | 11,300 |
| $\rho_0'$ | g/cm$^3$ | $4{\cdot}44 \times 10^{-3}$ | $3{\cdot}84 \times 10^{-3}$ |
| $p_0'$ | atm. | 115 | 205 |
| $i_0'$ | kcal/g | 4·25 | 9·29 |
| $\alpha$ | — | 0·6899 | 0·6899 |

TABLE 2. Stagnation conditions for oxygen and nitrogen

It will be remembered from the previous section that $\Phi$ probably lies within the range

$$3 \times 10^8 \leqslant \Phi \leqslant 3 \times 10^{13}.$$

The method of solution for the smaller values of $\Phi$ was to start integration upstream of the throat, and to seek by trial and error for a mass flow rate $\rho^* v^*$ which satisfied the condition $v = c$ at the critical point just downstream of the throat. The solution could then be continued downstream of the critical point using this value of $\rho^* v^*$. This trial and error procedure turned out not to be necessary with the larger values of $\Phi$ for which the flow was still essentially in equilibrium at the critical point. The step-by-step integration was therefore started from equilibrium in these cases, at a point just downstream of the critical point, using the equilibrium value of $\rho^* v^*$. It was found that the exact initial point for these integrations did not materially affect the solution further downstream. However, the interval size had to be very small in order to prevent the step-by-step integration from diverging, and so the computing times were long, especially for the larger values of $\Phi$. To reduce this time to a minimum a computational programme was devised which periodically chose the largest possible

interval satisfying the condition that the integration error had to be less than a specified amount.

Some of the results of these calculations are shown in figures 2 to 7. The dissociation fraction $\alpha$ is plotted against the nozzle area ratio $A$ in figure 2 for the limiting cases of frozen flow ($\Phi = 0$) and equilibrium flow ($\Phi = \infty$), and for three typical

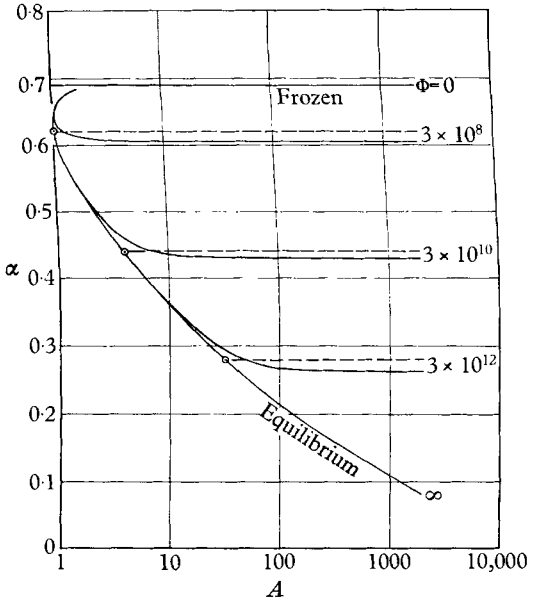


FIGURE 2. The dissociation fraction. Stagnation conditions: $T_0 = 0{\cdot}1$, $p_0 = 5 \times 10^{-6}$, $s = 0$. ———, Exact solutions; — — — —, approximate solutions.

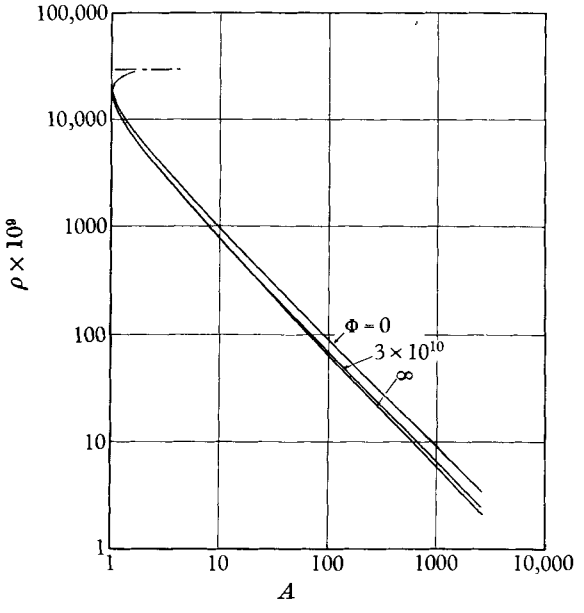


FIGURE 3. The reduced density. Stagnation conditions: $T_0 = 0{\cdot}1$, $p_0 = 5 \times 10^{-6}$, $s = 0$.

intermediate cases: $\Phi = 3 \times 10^8$ (Southampton University tunnel, Wood's rate constant for oxygen); $\Phi = 3 \times 10^{10}$; and $\Phi = 3 \times 10^{12}$ (16 in. 'Hotshot' tunnel, Heims's rate constant for oxygen). The parameter $s$ is taken to be zero throughout. The intermediate solutions are initially indistinguishable from the equilibrium case in the upstream part of the nozzle, as predicted in the previous section; but, once a significant departure from equilibrium has begun, $\alpha$ very soon approaches

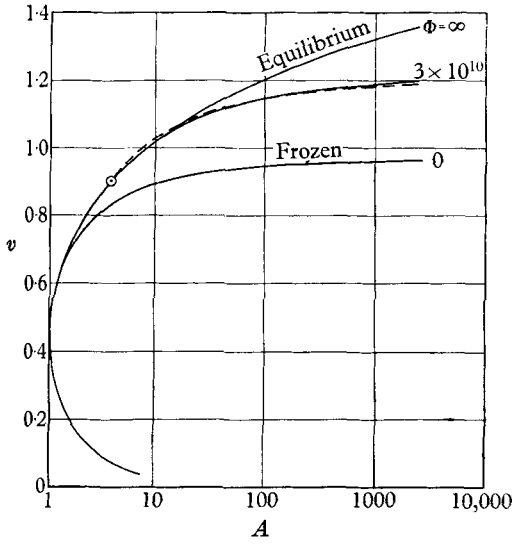


FIGURE 4. The reduced velocity. Stagnation conditions: $T_0 = 0{\cdot}1$, $p_0 = 5 \times 10^{-6}$, $s = 0$. ———, Exact solutions; — — —, approximate solution.

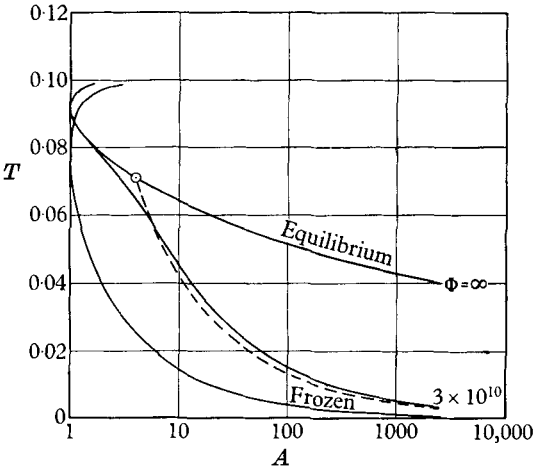


FIGURE 5. The reduced temperature. Stagnation conditions: $T_0 = 0{\cdot}1$, $p_0 = 5 \times 10^{-6}$, $s = 0$. ———, Exact solutions; — — —, approximate solutions.

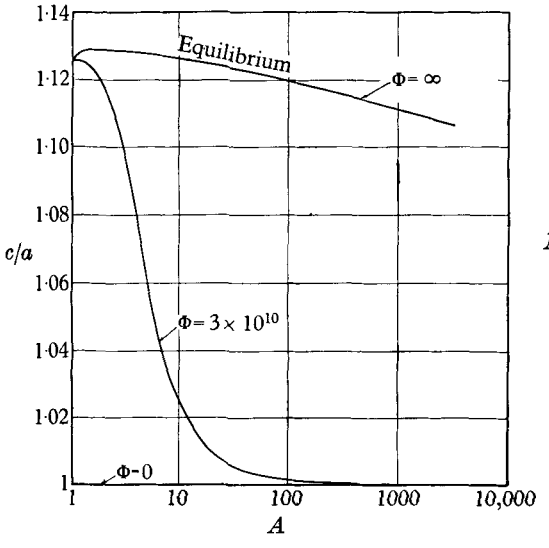


FIGURE 6. The ratio of characteristic speed to sound speed. Stagnation conditions: $T_0 = 0{\cdot}1$, $p_0 = 5 \times 10^{-6}$, $s = 0$.

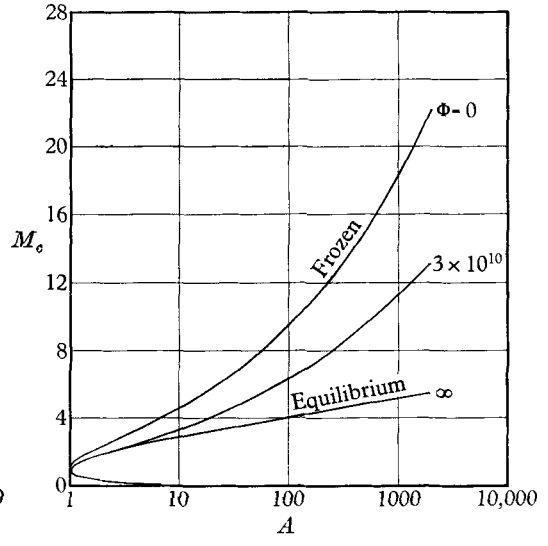


FIGURE 7. The Mach number. Stagnation conditions: $T_0 = 0{\cdot}1$, $p_0 = 5 \times 10^{-6}$, $s = 0$.

a constant value and does not change further, no matter how large $A$ may become. This behaviour is also to be expected from the form of the rate equation (15), which in the downstream part of the nozzle is dominated by the recombination term, so that

$$\frac{d\alpha}{d\xi} \simeq -\Phi\rho^2\left(\frac{T}{T_0}\right)^{-s}\frac{\alpha^2}{v}.$$

The density is becoming very small in this region (see figure 3), and so $d\alpha/d\xi$ must become small also; in fact, the velocity is almost constant at its limiting value so that $d\alpha/d\xi$ approaches zero roughly as $A^{-2}$. Once the flow has become frozen in this manner, equation (15) suggests that there is no chance of it unfreezing again further down the nozzle unless $s$ is very large. Note that this behaviour is a direct result of the three-body collision process which is required for recombination; if recombination takes place in this way, then the $\rho^2$ term will always occur, whatever the details of the recombination equation. Presumably $d\alpha/d\xi$ will always become small if the density is sufficiently low.

Figures 3, 4 and 5 show respectively the dimensionless density, velocity and temperature plotted against the area ratio for the cases $\Phi = 0$, $3 \times 10^{10}$ and infinity, with $s = 0$. As before, the intermediate solution starts off from equilibrium and then quite suddenly diverges towards the frozen solution. The solutions for other values of $\Phi$ are not shown on these graphs as they behave in an exactly similar manner; the case with $\Phi = 10^6$ is hardly distinguishable from frozen flow. The ratio of the characteristic speed $c$ of equation (19) to the sound speed $a$ (equation (16)) has been calculated for the same cases, and is shown in figure 6; for equilibrium flow this ratio remains nearly constant, while for frozen flow it is always unity. The intermediate case drops sharply from the equilibrium curve as freezing occurs. Figure 6 shows that the maximum error in using $c$ instead of $a$ is always less than 13 %, and will be almost zero in the test section after freezing has occurred. Because this error is small, $c$ rather than $a$ has been used to define a Mach number $M_c = v/c$, and this is shown in figure 7. Freezing causes a large increase in Mach number, because of the fall in temperature.

Integrations have also been carried out with various non-zero values of the parameter $s$, and figure 8 shows the variation of $\alpha$ with $A$ when $s$ takes the extreme value of 2·5, with the same stagnation conditions as were considered previously. It will be seen that the gas behaviour is qualitatively the same as for $s = 0$, with freezing taking place at the downstream end of the nozzle. However, the limiting value of $\alpha$ is somewhat smaller, and the approach to it is more gradual, as would be expected from the form of the rate equation. The effect of $s$ upon the dissociation fraction is seen to be comparatively small.

Another feature of the calculations is that the flow at the nozzle throat ($\xi = 0$) is very nearly in equilibrium for all the cases considered, except for $\Phi = 0$ and $10^6$. This means that the mass flow rate $\rho^*v^*$ is independent of $\Phi$ if $\Phi$ is sufficiently large. Actually, $\rho^*v^*$ does not vary greatly, even as $\Phi \to 0$, the limiting values being:

$$\Phi = 0, \quad \rho^*v^* = 0{\cdot}868 \times 10^{-5};$$

$$\Phi = \infty, \quad \rho^*v^* = 0{\cdot}797 \times 10^{-5}.$$

Penner (1955) has considered the one-dimensional flow of reacting gas mixtures for application to propellant systems such as rocket engine nozzles. His fundamental equations are similar to equations (12) to (15), but he goes on to develop two linearized treatments for near-equilibrium and near-frozen flows. In the first of these he assumes that the temperature $T$ in the relaxing flow is so close to the corresponding equilibrium temperature $T_e$ that an effective equilibrium constant may be defined for the relaxing flow as the first two terms of a Taylor series expansion about $T_e$. This requires that

$$\frac{T_e - T}{T_e} \ll 1.$$

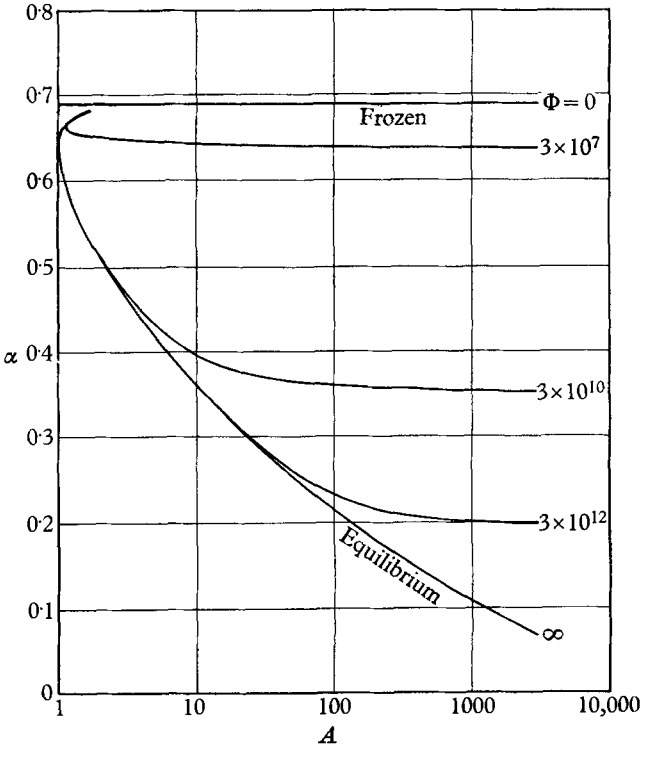


FIGURE 8. Effect of taking $s = 2{\cdot}5$ on the dissociation fraction. Stagnation conditions: $T_0 = 0{\cdot}1$, $p_0 = 5 \times 10^{-6}$, $s = 2{\cdot}5$.

Assuming that the approximation will become invalid if this fraction is greater than 0·5, then if $A = 1000$, $T_0 = 0{\cdot}1$ and $p_0 = 5 \times 10^{-6}$, we find that $\Phi$ must be greater than $2 \times 10^{13}$. Similarly, Penner gives a near-frozen solution, for which

$$\frac{T - T_f}{T_f} \ll 1,$$

where $T_f$ is the temperature for a given $A$ with $\Phi = 0$. Assuming again that this fraction must be less than 0·5, we find, for the case quoted above, that $\Phi$ must be less than $3 \times 10^7$. It appears, therefore, that there may be a wide range of values of the rate parameter $3 \times 10^7 < \Phi < 2 \times 10^{13}$

in which these approximate solutions can given appreciable errors.

For the rocket nozzle case it is permissible to neglect density changes in the nozzle when evaluating criteria for near-equilibrium and near-frozen flow (Penner 1955), but this approximation is grossly in error in the case of a hypersonic wind tunnel, as figure 3 shows.

## 5. Approximate solutions

The solutions of equations (22) and (23) which have been described in the last section all have the property that they are indistinguishable from the equilibrium solution (equations (26) and (27)) at points sufficiently far upstream. Figure 2 shows that the larger the value of $\Phi$ the further downstream will the deviations from equilibrium occur, but that once such a deviation begins $\alpha$ very soon reaches a constant value $\alpha_\infty$, say. In other words the flow becomes frozen, and the rate equation is approximately $d\alpha/dt = 0$.

Three flow regions may therefore be distinguished:

(1) A region of flow near to equilibrium, in which both the rate of dissociation $r_D$ and the rate of recombination $r_R$ are very large in comparison with the net dissociation rate $d\alpha/dt = r_D - r_R$, so that the equilibrium condition $r_D = r_R$ is closely satisfied. Equilibrium will then continue so long as this situation is maintained, that is so long as

$$-\frac{d\alpha}{dt} \ll r_D. \tag{29}$$

(2) A transition region, in which $\rho$ and $T$ have fallen sufficiently so that $r_D$ and $r_R$ are of the same order as $d\alpha/dt$, and there is consequently an appreciable departure from equilibrium. This results in an increase in the rate of fall of temperature, which reduces $r_D$ because of the exponential term and so increases the deviation from equilibrium. Once this process has begun, freezing takes place quite rapidly.

(3) A region of almost frozen flow, in which the exponential decrease of $r_D$ has gone so far that this term is negligible, i.e.

$$-\frac{d\alpha}{dt} \gg r_D \tag{30}$$

and consequently

$$-\frac{d\alpha}{dt} \simeq r_R.$$

But $r_R$ is proportional to $\alpha^2\rho^2$, if $s$ is small, and so approaches zero faster than $A^{-2}$. The overall change of $\alpha$ in this region is small.

The two inequalities of equations (29) and (30) are the conditions for the gas to be near equilibrium and nearly frozen respectively. Freezing will take place suddenly if they are satisfied at adjacent points in the flow, and this will happen if $r_D$ is decreasing much more rapidly than $r_R$ as $\xi$ increases. From the definitions of $r_D$ and $r_R$, this means that $(1-\alpha)\,e^{-1/T}$ must approach zero faster than $\alpha^2\rho$, which is simply the condition that the gas shall not follow the law of mass action (equation (7)). Freezing reduces $T$ and increases $\rho$, and the sudden nature of the change appears to be due to the exponential form in which $T$ occurs in $r_D$.

If the transition from equilibrium to frozen flow does take place within a small region of the nozzle, then it should be possible to construct an approximate solution of the flow problem, in which freezing is assumed to occur instantaneously at a particular point. The following is a simple attempt to define this point of sudden freezing.

Since $(-d\alpha/dt)$ is much smaller than $r_D$ for equilibrium, and much larger than $r_D$ when the flow has frozen, somewhere in the freezing region the two quantities must be of the same order of magnitude. Very approximately,

$$-\frac{d\alpha}{dt} = Kr_D$$

at the freezing point, where $K$ is an undetermined constant, which we may expect to be of order unity. Now up to this point the gas is assumed to be in complete equilibrium, so that $d\alpha/dt$ and $r_D$ may be found from the equilibrium solution (equations (26) and (27)), and the equation for the freezing point becomes

$$-\left(\frac{d\alpha}{dt}\right)_e = Kr_{D_e}, \tag{31}$$

where the suffix $e$ denotes equilibrium. Equation (31) has been used to find the freezing point for the cases which were solved by step-by-step integration in the previous section, and approximate solutions for the region downstream of the freezing point have been computed by setting $\Phi = 0$, so that equation (25) applies. The results of some of these calculations are compared with the more accurate integrations in figures 2, 4 and 5, from which it appears that the approximation gives reasonable results in these cases. The constant $K$ has been taken equal to unity; actually, better agreement with the more accurate calculations is obtained if $K$ is 1·6, but the method probably does not warrant such accuracy since $K$ may actually vary. The results do not depend critically on the value chosen.

Equation (31) also gives the limiting value of the dissociation fraction, $\alpha_\infty$, as $A$ goes to infinity, and this is shown in figures 9 and 10, plotted against the rate parameter $\Phi$ for a wide range of stagnation conditions with $s = 0$. Figure 9 also gives the values of $\alpha_\infty$ determined from the numerical integrations of the previous section and the results of two further numerical integrations at $T_0 = 0{\cdot}08$ and $0{\cdot}12$ to check the predicted temperature variation of $\alpha_\infty$. Once again, agreement with the approximate results is quite good. The variation of $\alpha_\infty$ with $s$ is shown in figure 11; here the agreement between the approximate theory and the numerical integrations is not so good, suggesting that larger values of $K$ are required for $s$ greater than zero. The overall variation of $\alpha_\infty$ with $s$ is shown to be small, but this does have a noticeable effect on the value of $\Phi$ required to maintain equilibrium, which may be decreased by a factor of about ten if $s$ is changed from zero to 2·5.

It appears from figure 9 that if $s = 0$ the flow will be approximately frozen everywhere if $\Phi$ is less than $10^6$, and that it will be near to equilibrium everywhere if $\Phi$ is greater than a value $\Phi_e$, which varies from the region of $10^{14}$ with $T_0 = 0{\cdot}07$ to more than $10^{18}$ with $T_0 = 0{\cdot}15$. Anywhere within these very wide

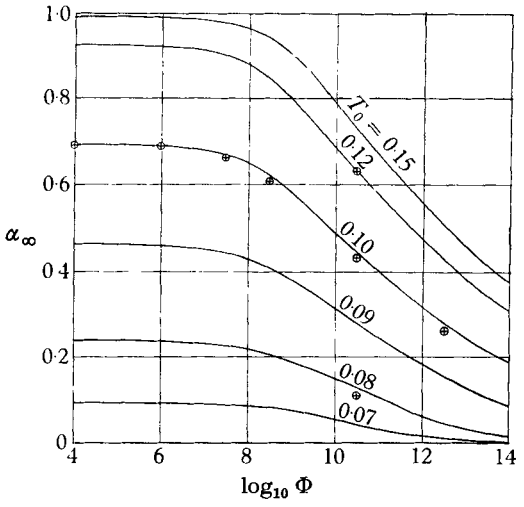


FIGURE 9. Limiting value of the dissociation fraction—effect of temperature. $p_0 = 5 \times 10^{-6}$, $s = 0$. ————, Approximate solutions; ⊕ ⊕ ⊕ ⊕, exact solutions.

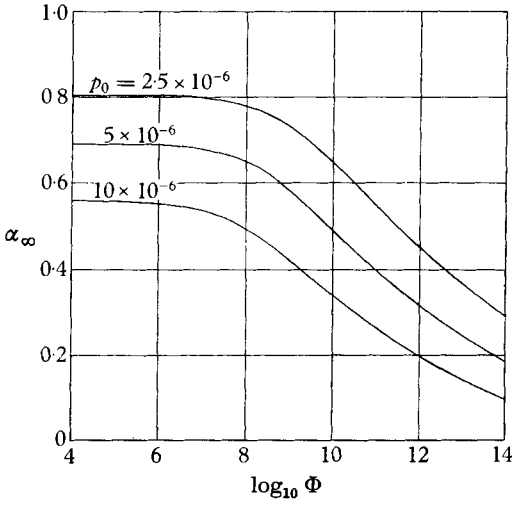


FIGURE 10. Limiting value of the dissociation fraction—effect of pressure. $T_0 = 0{\cdot}1$, $s = 0$, approximate solution.

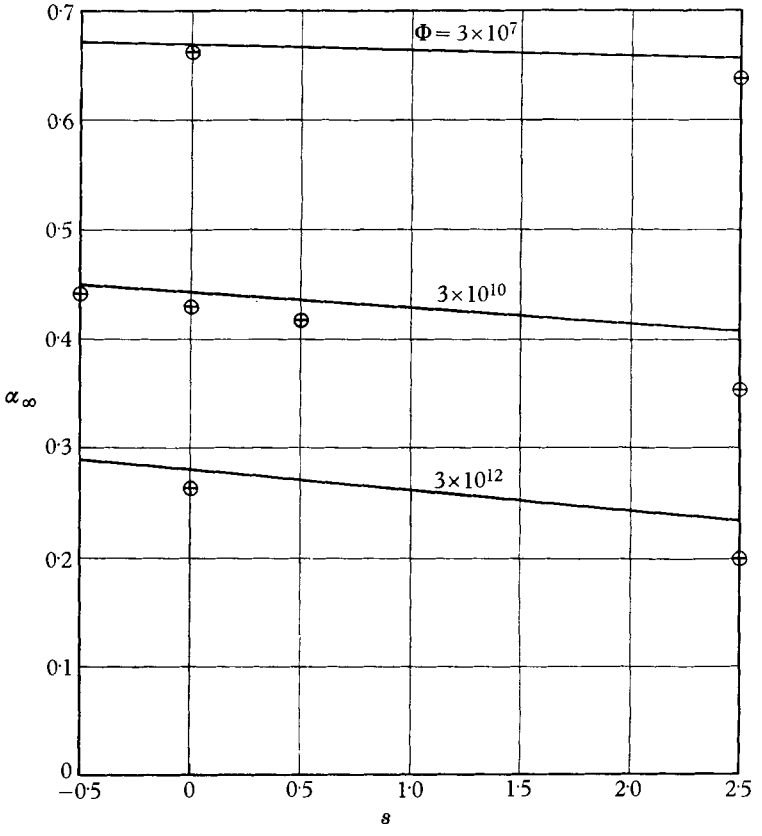


FIGURE 11. Limiting value of the dissociation fraction—effect of $s$. Stagnation conditions: $T_0 = 0{\cdot}1$, $p_0 = 5 \times 10^{-6}$. ————, Approximate solutions; ⊕ ⊕ ⊕, exact solutions.

limits the gas will be partly frozen and partly in equilibrium. It follows that nozzle scale effects must be small, since $\Phi$ is directly proportional to the linear dimensions of the nozzle, and increasing the nozzle size by a factor of ten cannot reduce $\alpha_\infty$ by more than about 0·1 at the most, while the reduction may be very much less. Also, we do not need to determine $\Phi$ very accurately in order to estimate how much freezing will take place in a particular nozzle; this is fortunate in view of the present uncertainty about dissociation and recombination rates.

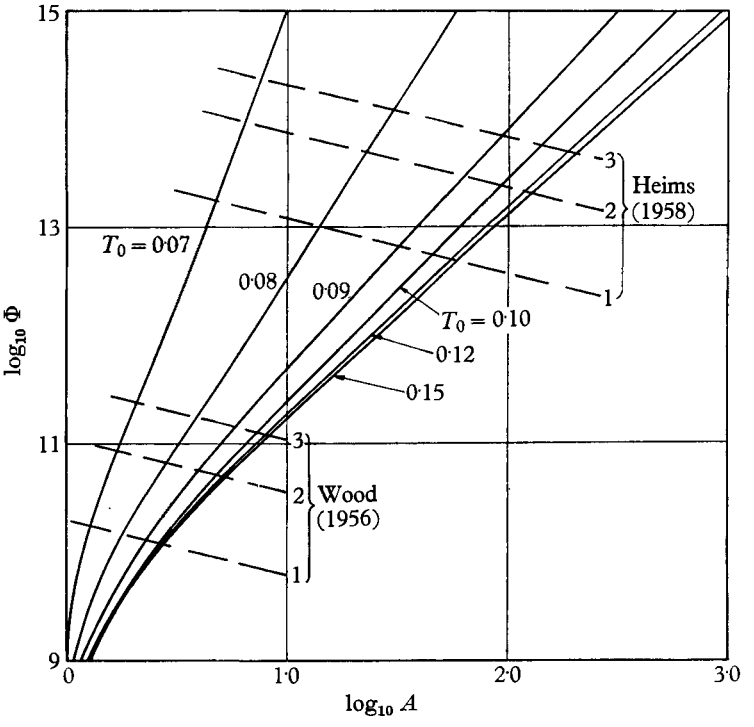


FIGURE 12. The rate parameter and area ratio for sudden freezing. 1, Southampton hypersonic tunnel; 2, 16 in. hotshot; 3, 50 in. hotshot. Approximate solutions: $p_0 = 5 \times 10^{-6}$, $s = 0$.

Figure 12 shows the area ratio at which the sudden freezing of this approximate theory will occur as a function of $\Phi$ for various temperatures. Also indicated are values of $\Phi$ using the rate constants of Woods (1956) and Heims (1958) for typical large and small nozzles. The intersections between the two sets of curves show the area ratios to which equilibrium may be maintained under various conditions.

The effect of stagnation pressure on the freezing process is shown in figure 10. Decreasing the stagnation pressure increases the value of $\Phi$ necessary for equilibrium; this will be important in low density high Mach number wind tunnels.

The above calculations have been concerned with the flow of a dissociating gas through a wind-tunnel-type nozzle, in which gas initially at rest is accelerated to hypersonic speed through a convergent-divergent nozzle with a sonic throat. However, there is interest also in the case of the hypersonic shock tube. Here the air is accelerated to a low supersonic speed by the passage of a strong normal

shock wave; it probably has time to reach thermodynamic equilibrium before it enters the divergent nozzle, and is accelerated to hypersonic speed. Under certain circumstances then, the shock-tube flow will be nearer to equilibrium than the corresponding wind-tunnel flow. However, from the calculations above it appears that if $\Phi$ is sufficiently large the wind-tunnel flow will also be in equilibrium at the point corresponding to the inlet of the shock-tube nozzle, and the two flows will then be identical downstream. This will occur if $\Phi$ is greater than $10^{10}$, approximately, for the cases considered here with $s = 0$.

It is possible that an equation similar to equation (31) may be useful to determine the conditions under which the flow of a real dissociating gas through a nozzle will freeze.

## 6. Effects of nozzle shape: the optimum nozzle

Any conical nozzle is included in the above analysis, and the expansion angle does not appear explicitly in the results, as it is contained in the dimensionless rate parameter $\Phi$. However, a wind tunnel working section is usually a duct of constant cross-sectional area, and this case needs special consideration.

We have shown in previous sections that, if $\Phi$ lies within a certain wide range of values, the dissociation fraction $\alpha$ will approach a constant value $\alpha_\infty$ in the expanding part of the nozzle, and that the recombination rate, $-d\alpha/dt$, will become small. In this section we shall try to determine whether it is possible for $-d\alpha/dt$ to become larger again in a region of parallel flow, and hence whether $\alpha$ can deviate from $\alpha_\infty$ in such a region. We shall also consider the problem of finding an optimum nozzle shape to avoid freezing as far as possible.

It is assumed that the transition to parallel flow takes place smoothly and in a short distance, so that the flow conditions at the beginning of the constant area region are the same as those at the end of the expansion. The rate equation (15) then shows that $-d\alpha/dt$ will be the same at both ends of this transition region. We wish to discover how rapidly $-d\alpha/dt$ can vary downstream of this point, and an upper limit to this variation is given by neglecting the rate of dissociation entirely, so that equation (15) becomes

$$-\frac{d\alpha}{dt} = C\rho^2\left(\frac{T}{T_0}\right)^{-s}\alpha^2.$$

Now $\rho$ is proportional to $1/v$, since the area is constant, so if $s = 0$,

$$-\frac{d\alpha}{dt} \sim \left(\frac{\alpha}{v}\right)^2$$

The temperature is low in the working section, so equations (9) and (14) give

$$v^2 \simeq 2(i_0 - \alpha)$$

and

$$-\frac{d\alpha}{dt} \sim \left(\frac{\alpha}{i_0 - \alpha}\right)^2.$$

This shows that $-d\alpha/dt$ gets smaller as $\alpha$ gets smaller; in fact, at the entrance to the constant area portion of the nozzle, $-d\alpha/dt$ is already small, and it must become still smaller downstream, so there appears to be no likelihood of an

appreciable change in $\alpha$ taking place within this region if $s = 0$. Putting $s = \frac{1}{2}$ multiplies all values of $d\alpha/dt$ in the above argument by a factor of about 5 for the cases considered in §4, but this is not nearly enough to affect the numerical value of $\alpha$ significantly.

It appears, then, that freezing will eventually take place in a nozzle of the type considered, and that a constant area working section will not unfreeze the gas appreciably. However, it is still possible that there is a different nozzle shape which will give better results.

The maintenance of equilibrium in a nozzle depends not only on the rate constant of the gas passing through it, but also on the size and shape of the nozzle itself. These factors have been combined in the dimensionless rate parameter $\Phi$, which determines whether the flow remains in equilibrium or how soon it freezes. For conical nozzles $\Phi$ may be written in the form

$$\Phi = BA^{\frac{1}{2}} \Big/ \frac{dA}{dZ}, \tag{32}$$

where $B$ is a reduced reaction rate constant, $C\sqrt{\left(\frac{A^*}{D/2m}\right)}$, and $Z$ is the ratio $x'/\sqrt{A^*}$, where $x'$ is the distance along the nozzle axis.

The area ratio at which sudden freezing will occur has been calculated from equation (31) as a function of $\Phi$ for different stagnation conditions. The results are shown in figure 12. They enable us to estimate the minimum value of $\Phi$ required to expand a given flow through a given area ratio in a conical nozzle and maintain equilibrium. If the gas properties are known, equation (32) then gives the maximum allowable expansion angle for the nozzle. In practice this angle usually turns out to be very small, giving a conical nozzle which is much too long, and a test section flow which is filled by the wall boundary layer.

We therefore wish to find the shape of a nozzle which will expand the flow from a given throat area to a given test section area in the shortest possible length, consistent with the maintenance of thermal equilibrium, in order to cut down boundary layer growth. This will be called an optimum nozzle in the following paragraphs.

The optimum nozzle has a shape which keeps the flow continually on the verge of freezing, but never expands it quite fast enough for freezing to occur. Such a shape will clearly start with a large expansion angle near the throat where the temperature and density are high so that the rate of recombination may be large, but the expansion angle will get progressively less further down the nozzle.

A very approximate expression for this shape may be found by regarding the optimum nozzle as being made up of a large number of conical sections, in each of which the expansion angle is chosen so that $\Phi$ is large enough to ensure equilibrium. Then, from equation (32), the optimum shape is given by

$$Z = \frac{1}{B}\int_1^{A_t} \frac{\Phi(A)}{A^{\frac{1}{2}}}\, dA, \tag{33}$$

where $\Phi(A)$ is the rate parameter required to maintain equilibrium, which may be obtained from figure 12. The equation of the corresponding conical nozzle, having

the same value of $\Phi$ at its exit area $A_t$, and therefore giving the same test section conditions providing both nozzles do in fact maintain equilibrium, is

$$Z = \frac{2}{B}\Phi(A_t)A^{\frac{1}{2}}.$$

Now the data of figure 12 is fitted quite well by an equation of the form

$$\Phi = \Theta A^n, \tag{34}$$

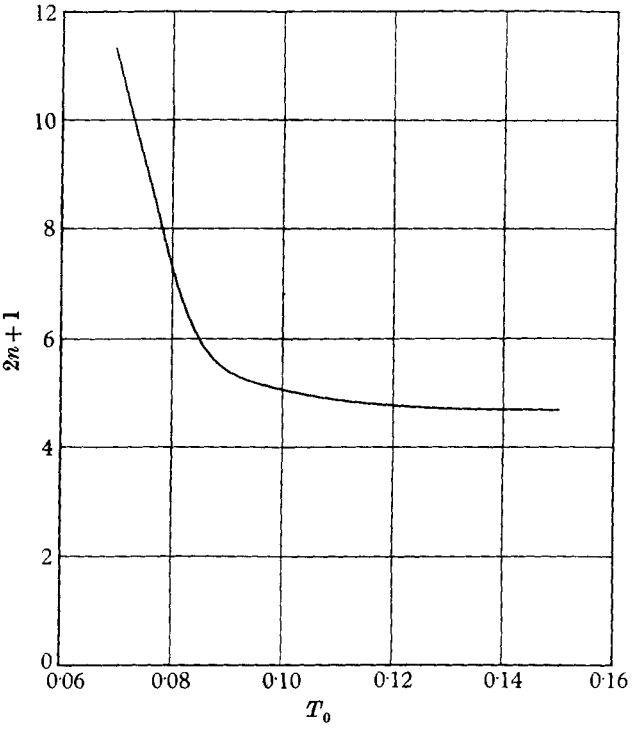


FIGURE 13. Ratio of length of conical nozzle to length of corresponding optimum nozzle. $p_0 = 5 \times 10^{-6}$, $s = 0$.

where the constants $\Theta$ and $n$ depend on the stagnation conditions. To this approximation the optimum nozzle shape, equation (33), becomes

$$Z = \frac{\Theta}{B}\frac{A^{n+\frac{1}{2}}}{n+\frac{1}{2}}, \tag{35}$$

and the ratio between the overall lengths of the conical and optimum nozzles is simply

$$\frac{(Z_t)_{\text{con}}}{(Z_t)_{\text{opt}}} = 2n+1. \tag{36}$$

This ratio is plotted in figure 13, against stagnation temperature, for the case $s = 0$. It will be seen that the optimum nozzle is between one-fifth and one-tenth of the length of the corresponding conical nozzle, which should lead to a worthwhile saving in boundary layer growth.

An analysis of this kind is obviously not mathematically rigorous and so needs checking. In order to carry out such a check a few step-by-step integrations have been made for nozzles of the shape given by equation (35), with the parameters $\Theta$

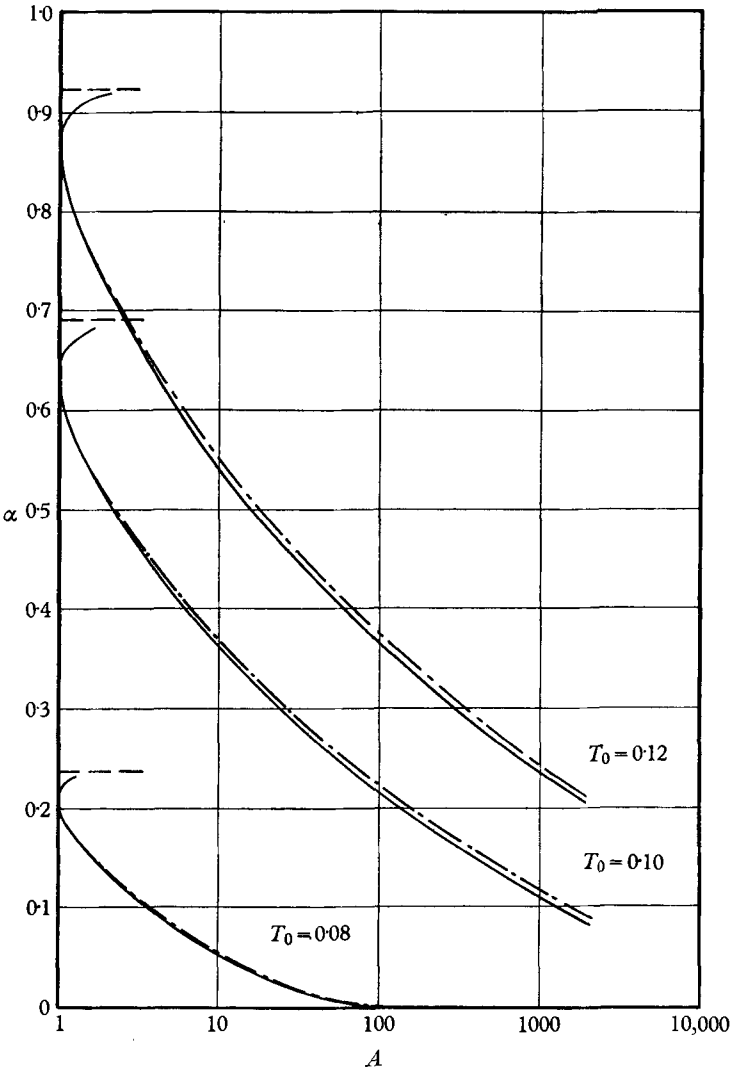


FIGURE 14. Dissociation fraction for optimum nozzles. Stagnation conditions: $p_0 = 5 \times 10^{-6}$, $s = 0$. ————, Equilibrium; —·—·—, optimum nozzle.

and $n$ taking the values indicated from figures 12 and 13. The dissociation fraction $\alpha$ obtained from these calculations for three different stagnation temperatures is compared with the corresponding equilibrium solutions in figure 14. It will be seen that a flow very close to equilibrium is achieved in each case. A numerical example of the size and shape of the optimum nozzle is given below for a typical case.

We consider a hypersonic wind tunnel with an area ratio of 1000. The working fluid is oxygen and the stagnation conditions are $T_0 = 0{\cdot}1$ and $p_0 = 5 \times 10^{-6}$ (corresponding to 5900° K and 115 atmospheres).

Figures 9 and 12 suggest that to ensure complete equilibrium in the test section of this tunnel the $\Phi$-value for its conical nozzle would have to be about $10^{15}$, if $s = 0$. Figure 1 then shows that the nozzle would need to be 630 m long, if the rate constant of Heims (1958) is used; the corresponding optimum nozzle would be 126 m long. If $s$ takes the extreme value of 2·5 the required $\Phi$ is reduced to about $10^{14}$, so the lengths of the conical and optimum nozzles are 63 and 12·6 m, respectively. An optimum nozzle for this case, with a test section area of two square metres, is drawn to scale in figure 15. Its shape requires some modification near the throat, which adds slightly to the length.

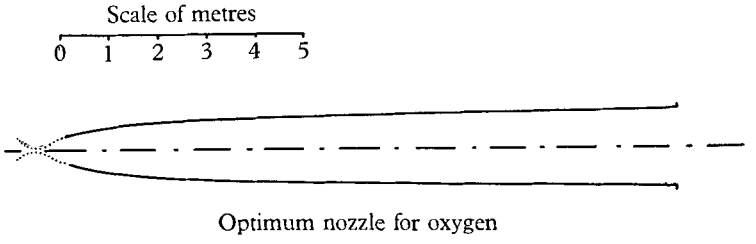


FIGURE 15. Shape of optimum nozzle. Stagnation conditions: $T_0 = 0{\cdot}1$, $p_0 = 5 \times 10^{-6}$, $s = 2{\cdot}5$.

Nozzles of this type might not be practical for aerodynamic reasons even if they were smaller. However, the calculations above do suggest that a modest decrease in dissociation fraction for a given nozzle length may be achieved by suitable contouring. The initial rate of expansion downstream of the throat must be as large as other considerations will allow, and then the rate of expansion must be progressively reduced further downstream.

## 7. Effects of lack of equilibrium in the test section

The calculations presented above suggest that the flow in the test section of a hypersonic wind tunnel may deviate considerably from thermal equilibrium for a wide range of stagnation conditions. We must therefore consider what effects these non-equilibrium phenomena will have on quantities measured in the tunnel test section.

Figure 16 shows the conditions that will be encountered at an expansion ratio of 1000 with $s = 0$, $T_0 = 0{\cdot}1$ and $p_0 = 5 \times 10^{-6}$ as calculated in § 4, plotted against the rate parameter $\Phi$. It will be seen that the velocity is slightly reduced by freezing and the density is correspondingly increased; however, the temperature is reduced by a factor of about 40 and the static pressure by about 17. These large changes may be expected to have a considerable effect on the flow past bodies in the tunnel. Most bodies at present being tested are more or less blunt-nosed and will therefore have nearly normal shock waves in front of them, so it is of interest to see what effect freezing in the flow upstream of a normal shock will have on the

flow behind it. If conditions ahead of the shock are denoted by a suffix (1) and those behind by (2), then the equations of motion are:

$$\rho_1 v_1 = \rho_2 v_2, \tag{37}$$

$$p_1 + \rho_1 v_1^2 = p_2 + \rho_2 v_2^2, \tag{38}$$

$$i_1 + \tfrac{1}{2} v_1^2 = i_2 + \tfrac{1}{2} v_2^2. \tag{39}$$

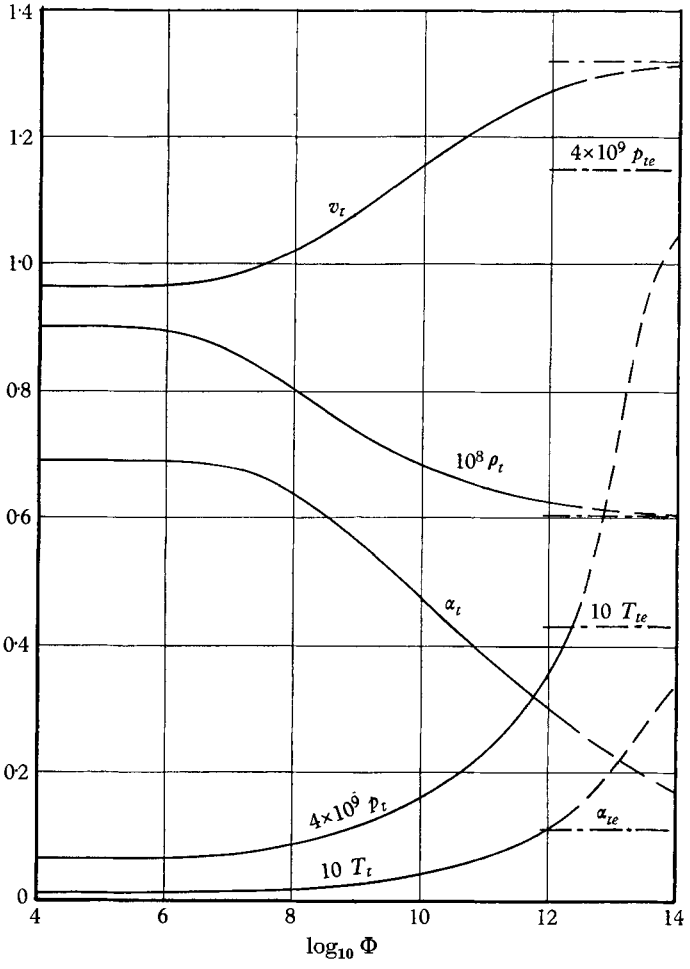


FIGURE 16. Test section conditions. $A_t = 1000$, $T_0 = 0{\cdot}1$, $p_0 = 5\times10^{-6}$, $s = 0$.

The conditions ahead of the shock are known from the nozzle calculations of §4 as functions of $\xi$ or $A$, so the shock wave equations can be solved at a given $\xi$. It is assumed for the present that equilibrium is reached quickly behind the shock, so that

$$\frac{\alpha_2^2}{1-\alpha_2} = \frac{1}{\rho_2} e^{-1/T_2}$$

from the law of mass action (equation (7)). This is a reasonable assumption, as the high temperature and pressure behind the shock will favour rapid equilibrium; however, relaxation effects behind the shock are discussed later in this section.

Using the thermodynamic relationships of § 2 and neglecting $p_1$, which must be very much smaller than $\rho_1 v_1^2$ if the flow is hypersonic, equations (37), (38) and (39) may be written:

$$\frac{\rho^* v^*}{A_1} = \rho_2 v_2, \tag{40}$$

$$\frac{\rho^* v^*}{A_1}\sqrt{[2(i_0 - i_1)]} = p_2 + \rho_2 v_2^2, \tag{41}$$

$$i_0 = i_2 + \tfrac{1}{2}v_2^2. \tag{42}$$

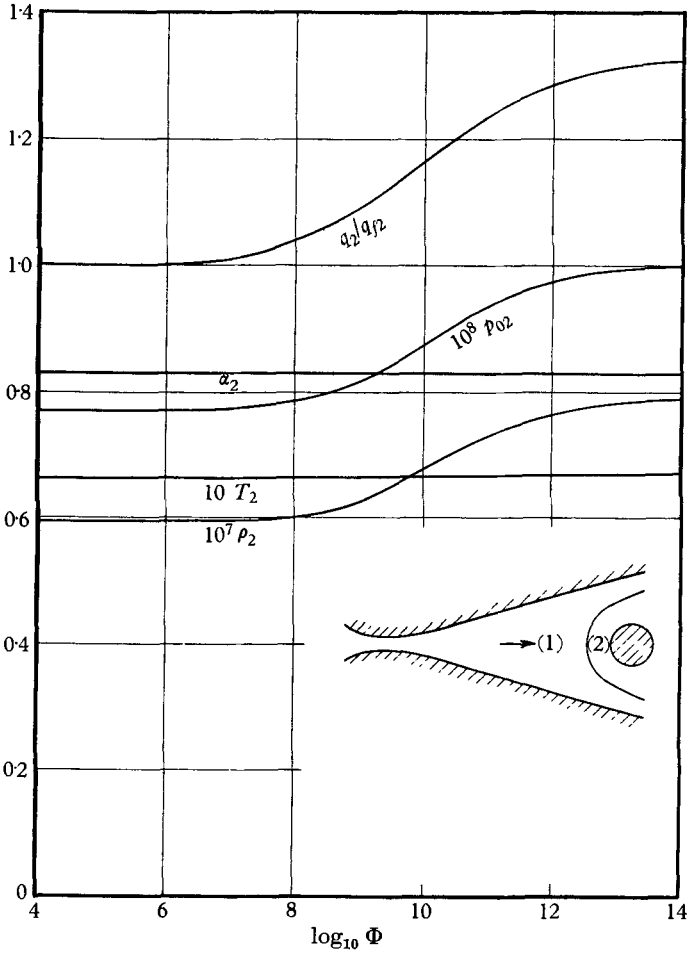


FIGURE 17. Conditions behind a normal shock wave. $A_1 = 1000$, $T_0 = 0{\cdot}1$, $p_0 = 5 \times 10^{-6}$, $s = 0$.

The left-hand sides of equations (40) and (42) are independent of nozzle relaxation effects, since we have shown that the mass flow $\rho^* v^*$ does not vary much with $\Phi$. The left-hand side of equation (41) does contain $i_1$, which depends on $\Phi$, but the numerical variation of the whole term is not large. Also, from equation (42), the enthalpy behind the shock, $i_2$, cannot differ greatly from the stagnation enthalpy, $i_0$, since the velocity behind a strong shock wave is small, so that $i_2$ must be almost independent of $\Phi$. It follows that the equilibrium

conditions behind a normal shock wave cannot be greatly affected by relaxation in the nozzle upstream of the shock.

Solutions of equations (37), (38) and (39) have been found by Lighthill's iteration method (Lighthill 1957) for the case with $s = 0$, $T_0 = 0{\cdot}1$, $p_0 = 5 \times 10^{-6}$ and $A_1 = 1000$, by using the results of §4, and the results of these calculations are shown in figure 17. It will be seen that $\alpha_2$ and $T_2$ are almost independent of the degree of freezing in the nozzle, but that freezing reduces the density behind the

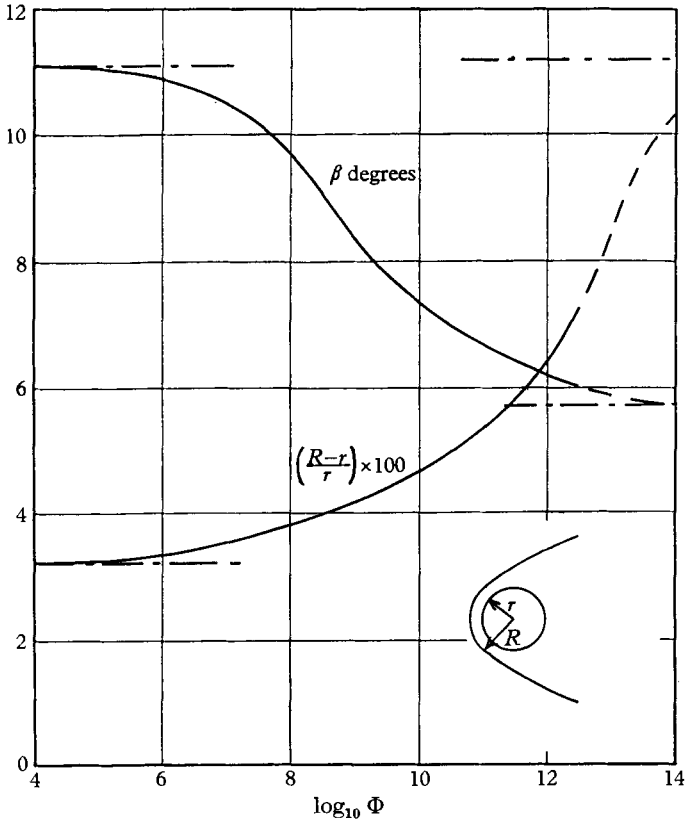


FIGURE 18. Mach angle and stand-off distance for a sphere. $A_1 = 1000$, $T_0 = 0{\cdot}1$, $p_0 = 5 \times 10^{-6}$, $s = 0$.

shock to about 75 % of its equilibrium value. The Pitot pressure, $p_{02}$, is also shown in figure 17, and it also is reduced somewhat by freezing. To the accuracy of the Newtonian approximation, the drag of a given body is proportional to the Pitot pressure, so the $p_{02}$ curve shows that drag forces will be underestimated in a frozen flow. An estimate of the effect of non-equilibrium in the nozzle on the heat transfer rate at the stagnation point of a blunt body can also be made. Fay & Riddell (1958) have solved the heat transfer problem for a wide range of conditions; here their solution for equilibrium within the boundary layer has been used together with the assumption of constant wall conditions, and figure 17 shows the calculated ratio of heat transfer rate ($q_2$) to heat transfer rate with $\Phi = 0$ ($q_{f2}$). Freezing in the nozzle is seen to cause a reduction in the measured heat transfer rate.

Further, the simple blunt body theory described by Lighthill (1957), in which the flow between the shock wave and the nose of the body is assumed to be incompressible, can be applied to determine the stand-off distance of a shock wave in front of a spherical nose (see figure 18). The stand-off distance depends on the shock wave density ratio; $\rho_2$ is reduced by freezing while $\rho_1$ is increased, and the resulting change in $\rho_2/\rho_1$ is sufficient to increase the stand-off distance by a factor of two as the flow freezes.

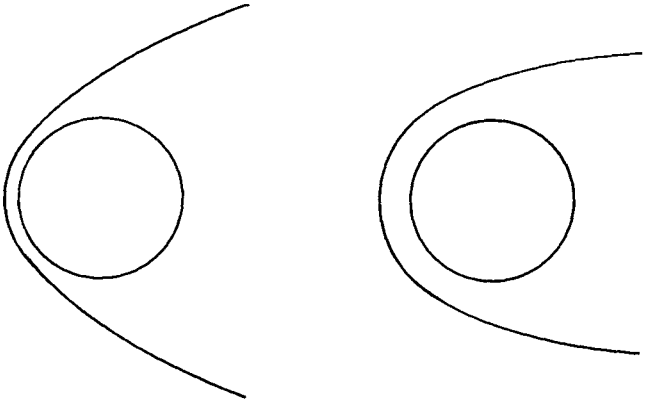


FIGURE 19. Shock wave shapes for equilibrium and frozen flow (not to scale).

According to approximations of the Newtonian type the shock wave in front of a blunt body closely follows the body shape near the front stagnation point, further round the body the shock separates from the surface, and after this its strength gradually weakens and its inclination gradually approaches that of a Mach wave. It is therefore of interest to calculate the Mach angle

$$\beta = \sin^{-1}\frac{c}{v},$$

and this has been done from the calculations of §4. The results are shown in figure 18, from which it will be seen that the Mach angle is reduced by a factor of about three if freezing occurs, mainly because of the large fall in static temperature. This result, together with the increase in stand-off distance, suggests that a measurable change in shock wave shape may be expected as a result of nozzle freezing. This effect is illustrated in the sketches of figure 19, which are not to scale.

The above analysis of flow past a blunt body neglects any lack of equilibrium in the flow between the shock wave and the spherical nose, but Freeman (1958) has provided the necessary extension to non-equilibrium flows. He shows that for a given set of equilibrium conditions upstream of the shock, the stand-off distance depends on a dimensionless rate parameter

$$\Lambda = \frac{2rCT_0^s}{\sqrt{(D/2m)}}\left(\frac{\rho_1}{v_1}\right) \tag{43}$$

in our notation, where $r$ is the radius of the sphere. The ratio of our rate parameter $\Phi$ to Freeman's $\Lambda$ is

$$\frac{\Phi}{\Lambda} = \frac{\sqrt{(A^*)}\, v_1}{4K_N r T_0^s \rho_1}.$$

Now for a typical model in a typical hypersonic wind tunnel, this ratio is of the order of $1/\rho_1$ (if $s = 0$), that is, about $10^8$. But Freeman shows that most of the relaxation effects behind the shock wave occur, for a typical example, in the range

$$0 \leqslant \Lambda \leqslant 100,$$

or approximately in the range

$$0 \leqslant \Phi \leqslant 10^{10}.$$

The nozzle flow will still be nearly frozen with $\Phi$ in this range, so that as the gas passes through the shock $\alpha$ only has to make the small change from $\alpha_0$ to $\alpha_2$; this should reduce the effects of relaxation behind the shock. If $\Phi > 10^{10}$, so that the nozzle flow is approaching equilibrium, then $\Lambda > 10^2$ and relaxation behind the shock is again negligible in its effect on the stand-off distance. It therefore seems reasonable to assume, as we did earlier in this section, that the stand-off distance, as measured in a hypersonic wind tunnel, depends only on relaxation effects in the wind-tunnel nozzle itself. However, Freeman's analysis could, if necessary, be modified to allow for a non-zero value of $\alpha_1$.

## 8. Conclusions

If the assumptions which have been made in this paper are accurate, then the flow of a partly dissociated gas through a hypersonic shock tube or wind-tunnel nozzle will remain in chemical equilibrium until a certain point in the nozzle is reached. Downstream of this point the gas will 'freeze' quite rapidly, so that its composition will remain almost constant if the flow is expanded further or passed through a constant area test section. It is suggested that this behaviour is a consequence of the triple-body collision process through which recombination occurs, and that freezing can be avoided only if the reaction rate parameter $\Phi$ is greater than a value $\Phi_e$. This is about $10^{15}$ for the typical case considered in §4, if the area ratio of the nozzle is 1000 and $s = 0$. Increasing the stagnation temperature or decreasing the stagnation pressure increases $\Phi_e$, but a positive value of $s$ decreases it. If $s$ is increased from zero to 2·5, $\Phi_e$ is reduced by a factor of about ten.

The values of $\Phi$ achieved for the flow of oxygen or nitrogen in large and small nozzles with various values assumed for the rate constant lie within the range

$$3 \times 10^8 \leqslant \Phi \leqslant 3 \times 10^{13},$$

so it is concluded that freezing will occur under conditions of practical interest.

The shape of an optimum nozzle has been derived in order to expand the gas in equilibrium in the shortest possible length. This is shown to be about one-fifth of the length of the corresponding conical nozzle, but it is still too long for practical applications.

The flow near the nose of a blunt body in the tunnel test section is shown to be affected only slightly by freezing in the nozzle, but the shock wave shape may be altered significantly.

Part of this work was carried out while the author was employed as a Vacation Consultant to the Ministry of Supply at the Armaments Research and Development Establishment, Fort Halstead, and was presented in an unpublished report (Bray 1958).

The author would like to thank the staffs of the Basic Research Division A.R.D.E., and the Department of Computation, University of Southampton, for their assistance with the numerical computations.

## REFERENCES

Boa-Teh Chu 1957 (Brown University Report—un-numbered) Wright Air Development Center Tech. Note 57–213.

Bray, K. N. C. 1958 *Aero. Res. Counc., Lond., Rep.* no. 19,983.

Bray, K. N. C., Pennelegion, L. & East, R. A. 1958 *Aero. Res. Counc., Lond., Rep.* no. 20,520.

Byron, S. R. 1957 Ph.D. Thesis. Cornell University.

Cox, R. N. & Winter, D. F. T. 1957 AGARD *Rep.* no. 139.

Duff, R. E. 1958 *Physics of Fluids*, **1**, 3.

Evans, J. S. 1956 *Nat. Adv. Comm. Aero., Wash., Tech. Note* no. 3860.

Fay, J. A. & Riddell, F. R. 1958 *J. Aero. Sci.* **25**, 2.

Freeman, N. C. 1958 *J. Fluid Mech.* **4**, 4.

Heims, S. P. 1958 *Nat. Adv. Comm. Aero., Wash., Tech. Note* no. 4144.

Hertzberg, A. 1957 *Cornell Aero. Lab., Rep.* no. AD-1052-A-5.

Lighthill, M. J. 1957 *J. Fluid Mech.* **2**, 1.

Logan, J. G. 1957 *Inst. Aero. Sci., Washington, Preprint* no. 728.

Lukasiewicz, J. 1958 Paper presented to 1st Int. Congress Aero. Sci. (Madrid).

Penner, S. S. 1955 *Chemical Reactions in Flow Systems.* London: Butterworths.

Resler, E. L. 1957 *J. Aero. Sci.* **24**, 11.

Rose, P. H. 1957 AVCO *Research Note* no. 37.

Smelt, R. 1955 *Proc. Conf. on High Speed Aero., Poly. Inst. Brooklyn.*

Wigner, E. P. 1939 *J. Chem. Phys.* **7**, 8.

Winter, D. F. T. 1958 *Arm. Res. Dev. Est., Fort Halstead, Memo.* (B) 62/58.

Wood, G. P. 1956 *Nat. Adv. Comm. Aero., Wash., Tech. Note* no. 3634.